# Instruments and Methods

# A new high-precision borehole-temperature logging system used at GISP2, Greenland, and Taylor Dome, Antarctica

GARY D. CLOW

*U.S. Geological Survey, Menlo Park, California 94025, U.S.A.*

RICHARD W. SALTUS

*U.S. Geological Survey, Denver, Colorado 80225, U.S.A.*

EDWIN D. WADDINGTON

*University of Washington, Seattle, Washington 98195, U.S.A.*

ABSTRACT. We describe a high-precision (0.1–1.0 mK) borehole-temperature (BT) logging system developed at the United States Geological Survey (USGS) for use in remote polar regions. We discuss calibration, operational and data-processing procedures, and present an analysis of the measurement errors. The system is modular to facilitate calibration procedures and field repairs. By interchanging logging cables and temperature sensors, measurements can be made in either shallow air-filled boreholes or liquid-filled holes up to 7 km deep. Data can be acquired in either incremental or continuous-logging modes. The precision of data collected by the new logging system is high enough to detect and quantify various thermal effects at the milli-Kelvin level. To illustrate this capability, we present sample data from the 3 km deep borehole at GISP2, Greenland, and from a 130 m deep air-filled hole at Taylor Dome, Antarctica. The precision of the processed GISP2 continuous temperature logs is 0.25–0.34 mK, while the accuracy is estimated to be 4.5 mK. The effects of fluid convection and the dissipation of the thermal disturbance caused by drilling the borehole are clearly visible in the data. The precision of the incremental Taylor Dome measurements varies from 0.11 to 0.32 mK, depending on the wind strength during the experiments. With this precision, we found that temperature fluctuations and multi-hour trends in the BT measurements correlate well with atmospheric-pressure changes.

## INTRODUCTION

We have developed a system capable of making high-precision (0.1–1.0 mK) temperature measurements in deep or shallow boreholes in remote polar regions. This developmental effort was largely motivated by the need to utilize very high-quality data when reconstructing past climate (surface-temperature) changes directly from the present-day subsurface temperatures measured in boreholes (Clow, 1992). The availability of high-precision temperature data may prove useful for a number of other studies as well, examples of which include attempts to detect shear heating at the base of an ice sheet and studies to improve our understanding of heat-transfer rates within the firn layer.

Paleoclimate reconstruction using borehole temperatures (BT), sometimes referred to as "paleothermometry", has now been used in a number of studies (e.g. Dahl-Jensen and Johnsen, 1986; Alley and Koci, 1989; MacAyeal and others, 1991; Shen and Beck, 1991; Wang, 1992; Firestone, 1995). This reconstruction

technique is completely independent of the stable-isotope proxy methods (Dansgaard and others, 1973) and thus provides complementary climate information. However, a significant problem with the paleothermometry method is that the derived surface-temperature histories are badly "smeared" in time. This is primarily a consequence of the heat-diffusion process. While it cannot be eliminated, the extent of the temporal averaging in the reconstructed surface temperatures can be minimized through optimal experimental design. Application of the Backus–Gilbert inverse methods to the paleoclimate-reconstruction problem demonstrates that our ability to *resolve* past climatic events can be optimized by reducing the random errors in the temperature measurements to no more than 0.1% of the climate signal we are attempting to detect (Clow, 1992). Thus, to enhance the ability to detect temperature changes of 1 K during the Holocene, the precision of the BT data needs to be 1 mK, or better. The connection between resolving power and data precision is illustrated in Figure 1; in this figure, the high-frequency line represents a hypothetical surface-temperature history

## Reconstructed Temperature History
### Noise σ = 0.01 K



### Noise σ = 0.001 K



### Noise σ = 0.0001 K
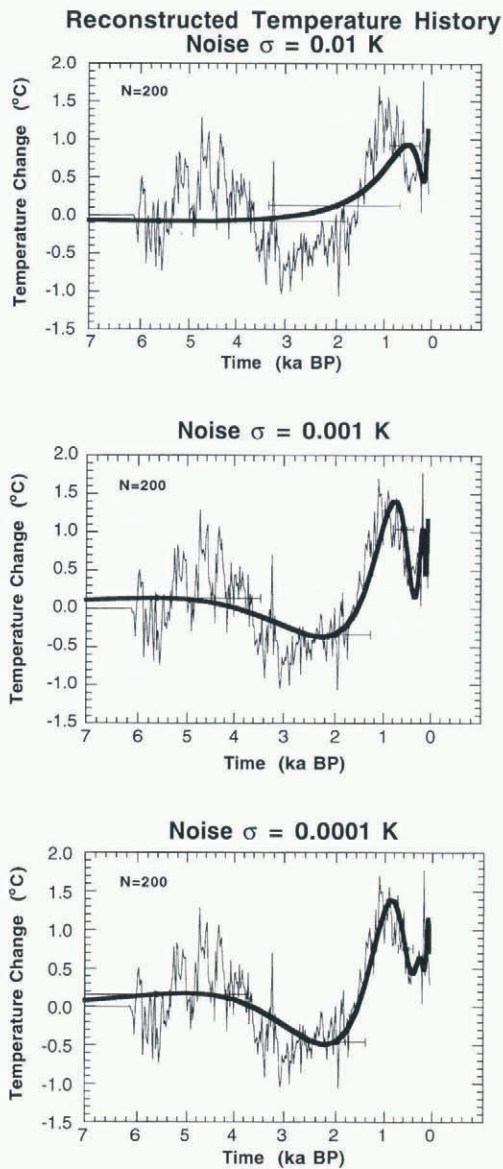


*Fig. 1. Temperature histories (bold lines) reconstructed from noisy synthetic borehole data. Noise levels are 10, 1 and 0.1 mK. The high-frequency line in each panel represents a hypothetical surface-temperature history used to calculate the synthetic borehole data. The mismatch between the hypothetical history and the reconstructed histories indicates the extent of the "temporal smearing" in the solutions; this is also indicated by the length of the horizontal lines at 560, 2000 and 5600 BP. A significant increase in resolving power is obtained by reducing the random errors in the borehole temperatures to the 1 mK level. 200 data points were used in these reconstructions.*

from which synthetic borehole temperatures have been calculated. The bold smooth line is the surface-temperature history reconstructed from the synthetic BT data for various levels of random noise. The improvement obtained by reducing the uncertainty in the temperature measurements from 10 to 1 mK is apparent.

Borehole temperatures differ from undisturbed ice temperatures due to two processes related to the presence of the hole. To quantify the effects of these processes and subsequently correct for them, the data precision must be high. The first process is the introduction of excess heat

into the hole by the drilling motor and by the drilling fluid. The effect is to disturb the temperature in the vicinity of the newly created hole. Repeat temperature logs can be used to assess the magnitude of the "drilling disturbance" and the rate at which it dissipates. This information can then be used in conjunction with a heat-transfer model to predict the equilibrium temperatures that will ultimately occur when the drilling disturbance vanishes. For mechanically drilled boreholes, the change in temperature as the drilling disturbance dissipates is often of order $10 \, \text{mK year}^{-1}$ or less within 1–2 years of hole completion. To evaluate and subsequently correct for the drilling disturbance within a few years of borehole completion, temperatures should be measured annually with a precision of at least 1 mK.

The second cause of thermal disturbance is the contrasting heat-transfer rates within a fluid-filled borehole and in the surrounding ice. Relative to the ambient ice, a borehole can act as a thermal insulator if the borehole fluid is stagnant, or as a "heat pipe" if the fluid is vigorously convecting. In either case, the isotherms are likely to be disturbed in the vicinity of the hole as heat preferentially follows the most efficient path. Temperature measurements with a precision 1 mK, or better, are required to determine convective heat-transfer rates within a borehole and hence to evaluate the extent to which isotherms are disturbed by the hole. This is particularly true of depths where the buoyant energy available to support fluid convection is marginal or where convection is fully turbulent.

Given the need for high-precision temperature measurements, we redesigned much of an existing U.S. Geological Survey (USGS) portable temperature-logging system to further reduce instrumental sources of measurement error. Calibration and operational procedures were also substantially modified. Our goal was to build a system capable of making borehole-temperature measurements under cold weather conditions with a precision better than 1 mK and an accuracy better than 5 mK. In this paper, we will: (1) describe the modified temperature-logging system and the associated measurement errors, and (2) present representative data recently acquired by this system at GISP2, Greenland, and at Taylor Dome, Antarctica. Data acquired by an earlier version of the logging system at GISP2 during 1992 are discussed in Saltus and Clow (1994) and Clow and others (1995).

## SYSTEM DESCRIPTION

Temperatures potentially can be measured in geophysical boreholes using vapor-pressure thermometers, radiation pyrometers, or simple thermocouples. However, most systems today utilize a temperature-dependent resistor (thermistor or RTD) whose resistance is measured by a commercial digital multimeter (DMM) or by a custom-built electronic bridge (see Beck and Balling, 1988). An advantage of a custom bridge is that it can be made small enough to be included in an instrument package located at the downhole end of the logging cable, keeping the electronic-lead lengths to the sensor relatively short. Such a package can be designed

to measure other parameters as well, such as fluid pressure and borehole inclination, with the resulting data either stored within the instrument package or transmitted to the surface through a cable with just two conductors. A significant disadvantage of this approach for precision temperature measurement is the difficulty of maintaining calibration of the electronic bridge because the temperature of the instrument package will often change by 10–30 K during a logging experiment. This can cause errors of 10 mK, or more, in the resulting temperature measurements. Although the use of a commercial multimeter on the surface potentially requires very long lead lengths (e.g. 3–4 km), the DMM can be maintained at a constant temperature, eliminating temperature-related drift in the resistance-measuring circuit. In addition, the DMM's calibration can be periodically rechecked while the measurements are in progress. With some systems, temperature measurements can be made while driving the sensor downhole at a constant speed ("continuous" logging), while with others, measurements can only be made when the probe is stopped at a fixed depth. The latter method, known as "incremental" or "stop-and-go" logging, results in a limited number of measurements at fixed depths. However, these measurements are free of the "slip-ring" noise (discussed later) inherent in continuous temperature logs. In addition, equilibrium temperatures can be directly measured using the incremental mode, eliminating the need to deconvolve the measured signal to account for the finite response time of the probe (Saltus and Clow, 1994).

When designing our logging system,[*] our priorities were high sensitivity, high accuracy, ruggedness and the ability to make measurements in either the continuous or incremental logging modes. With these priorities in mind, we decided to utilize negative-temperature-coefficient (NTC) thermistors for the temperature sensors and to measure their resistance using a commercial DMM residing on the surface. The DMM is wrapped in electronically controlled resistive heaters to maintain its operating temperature within a narrow range (22–24°C). Other major system components include a four-conductor logging cable mounted on a motorized rotating drum. A "slip-ring" assembly provides electrical continuity between the logging cable and the multimeter. Depth information is provided by an optical encoder mounted on a calibrated cable pulley. A laptop computer controls the system, both displaying and storing the resistance, depth, time and logging speed; resistance is converted to temperature during the data-processing step. The system is modular to facilitate system checks, to allow the use of different temperature sensors and to permit various logging cables to be used, depending on the depth of the hole. To minimize electrical noise, all components are battery-powered, except for the motor on our largest logging winch.

---

[*] The USGS has two primary temperature-logging systems. The system described in this paper is the one used for polar climate research.

## Resistance circuit

To measure the resistance of the temperature sensor, we use the four-wire circuit shown in Figure 2. During a four-wire measurement, the DMM produces a constant current $I_s$ which passes through the sensor. The voltage drop across the sensor is detected by the multimeter's high-impedance inputs, and the probe's resistance $R_s$ is calculated. This "four-wire resistance measurement", which is available on many commercial multimeters, automatically compensates for the resistance of the entire path between the DMM and the temperature sensor.
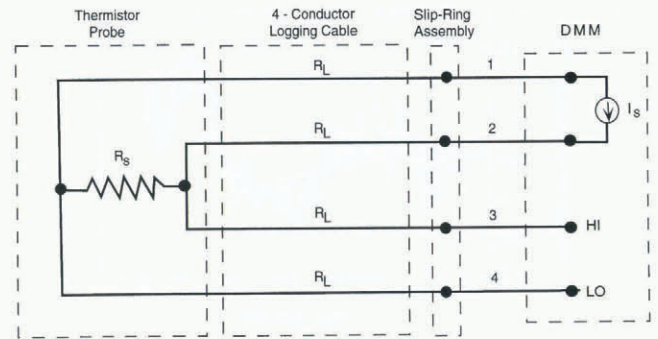
*Fig. 2. Four-wire resistance circuit utilized by the logging system. HI and LO are the high-impedance inputs of the DMM.*

With this circuit, the temperature sensitivity is simply

$$\Delta T \approx \frac{\Delta R}{\alpha_T R_s}, \qquad (1)$$

where $\Delta R$ is the smallest resistance resolvable by the multimeter, and $\alpha_T$ is the probe's temperature coefficient, defined by:

$$\alpha_T \approx \frac{1}{R_s} \frac{\partial R_s}{\partial T}. \qquad (2)$$

Typical $\alpha_T$ values for NTC thermistors range from $-0.04$ to $-0.07\,\mathrm{K}^{-1}$ at the temperatures encountered in polar ice sheets. In addition to using a high-quality DMM, we note that the system's sensitivity can be enhanced by using a probe whose resistance at the temperature being measured is near the high end of one of the resistance scales on the DMM.

Because the source current $I_s$ is generally quite small and the leads may be extremely long (e.g. 3–4 km), special attention must be given to various sources of noise and/or offset to prevent corruption of the data. These sources include: leakage paths between the circuit's electrical conductors, capacitance effects, self-heating effects, external electric fields, triboelectric effects, and switching effects.

Leakage paths between the conductors in the four-wire circuit can produce large errors, particularly when the sensor's resistance is large. Such unintended paths easily arise in the field due to broken or cracked insulation, or dirty connectors. Given an inter-conductor leak of resistance $R_l$, the error in the associated

temperature measurement is

$$\epsilon_1 = \frac{R_s}{\alpha_T(R_s + R_1)} . \qquad (3)$$

This problem can be controlled by cleaning the connectors, maintaining the integrity of the insulation and utilizing a probe with a small $R_s$ value. However, an additional constraint is that $R_s$ must be greater than the lead resistance $R_L$ for each leg of the four-wire circuit in order for an accurate resistance measurement to be made. As a rule of thumb, we find that $R_s$ should be at least 10 times $R_L$.

Because the logging cable has a capacitance $C$, the four-wire resistance circuit acts as a low-pass filter with a natural response time $\tau = R_s C$. Two issues arise here: (a) In order to properly record the changing probe resistance, $\tau$ must be much less than the time-scale for the resistance changes: $\tau \ll R_s(\partial R_s/\partial t)^{-1}$. (b) Assuming the condition in (a) is satisfied, small currents through the effective capacitance will still cause an error $\Delta R \approx \tau(\partial R_s/\partial t)$ in the resistance measurement. The associated error in temperature is

$$\epsilon_c = R_s C v \frac{\partial T}{\partial z} , \qquad (4)$$

where $v$ is the rate at which the probe descends into the borehole and $(\partial T/\partial z)$ is the local temperature gradient. The capacitance-related error $\epsilon_c$ can be minimized by keeping $R_s$ and $C$ relatively small, and by using a slow logging speed $v$.

As the source current $I_s$ from the multimeter passes through the temperature sensor, the probe will warm above the ambient-fluid temperature by an amount

$$\epsilon_h = \frac{I_s^2 R_s}{\delta} , \qquad (5)$$

where $\delta$ is the power-dissipation constant which depends both on the probe design and on the thermal properties of the fluid in which the measurements are being made. Corrections for this "self-heating" effect can be applied during the data-processing step since the current $I_s$ and the probe resistance $R_s$ are well known. However, the correct value for $\delta$ under field conditions is somewhat uncertain, so it is best to minimize the self-heating effect if possible. The best strategy is to use a multimeter that employs relatively small source currents and a probe specifically designed for minimal self-heating.

External electric fields can significantly disturb the measurements. Common sources are AC power fields near the resistance circuit, static charges near the multimeter inputs, and electric charges deposited on the sheath of the logging cable by dry blowing snow. We mitigate these problems by using shielded cables and by enclosing the multimeter in a shielded box. However, we are only partially successful because the shields cannot be properly tied to "ground" when working on an ice sheet. To further reduce these problems, we attempt to keep the entire system (including the logging cable) out of the wind whenever possible. The nylon tent surrounding the electronics package is enclosed in an insulating shell which minimizes charge build-up on the shelter; the

system operators (another significant source of static charge) remain several meters away from the multimeter during the course of an experiment, and all system components run off batteries rather than AC power. The only exception is our largest logging winch which is powered by 240 VAC. Although variations in the Earth's external magnetic field conceivably could induce currents in the logging cable, we have not seen evidence for such currents in multi-hour tests with the temperature sensor held at a fixed position in a buoyantly stable fluid.

Some of the noise we observe when a logging cable vibrates in the wind may be caused by the triboelectric effect (Keithley, 1984) in which charges are generated between the electrical conductors and the insulation as the cable flexes. Cables used to log boreholes filled with n-butyl acetate (Gosink and others, 1991) require Teflon insulation. Unfortunately, Teflon-insulated cables are known to be prone to this effect. Triboelectric noise may also occur as the logging cable flexes over the sheave wheels that guide the cable into the borehole. The triboelectric effect provides additional motivation to keep the logging cable out of strong winds.

Our dominant source of system noise in a continuous temperature log is caused by switching effects within the electromechanical "slip-ring" connector that provides electrical continuity between the logging cable and the DMM. Although we use a special slip-ring assembly to minimize this effect, the noise produced by the slip-ring connector is still generally of order 1 mK. As a final noise-reduction strategy, we use a multimeter that integrates the input signal for 100 ms for each measurement. This effectively eliminates high-frequency noise from all sources. A capacitor can also be introduced between the high-impedance inputs of the DMM to extend the range of the high-frequency filtering. The value of the capacitor must be chosen carefully so that the response time of the resistance circuit remains less than that of the temperature sensor and to limit the capacitance-related error $\epsilon_c$.

## Temperature sensors

From Equations (1)–(5), it is clear that the temperature sensor plays a significant role in determining the characteristics of the overall system. We currently use two sensor designs, one for immersion in liquid-filled boreholes and the other for measuring temperatures in air-filled holes. Both designs utilize multiple NTC bead thermistors to reduce the self-heating effect.

Our "polar" immersion probes[*] were custom-made by Fenwall Electronics. They consist of 15 thermistors divided into three packets, each of which is hermetically sealed in glass (Fig. 3). This prevents changes in the oxidation state of the metal-oxide thermistors and relieves strain where the leads are attached to the ceramic body of the thermistors. As a result, the probes have excellent

---

[*] A similar design appropriate for temperatures at mid-latitudes is described by Sass and others (1971). The mid-latitude version has a much higher resistance than the polar model and contains 20 thermistors divided into two packets.

**Immersion Probe**
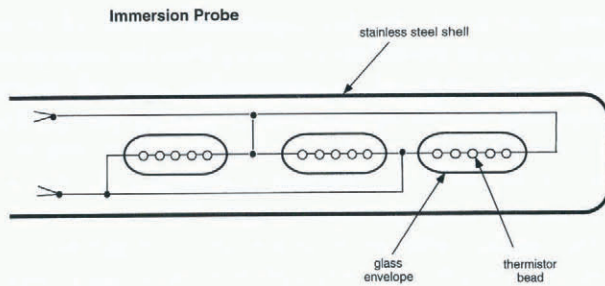


*Fig. 3. Temperature sensor for liquid-filled boreholes. The sensor contains 15 small bead thermistors divided into three packets; the use of multiple beads substantially reduces the "self-heating" effect. The beads extend over a ~10 cm length within a 4.0 mm diameter stainless-steel shell. The DMM measures the resistance of the entire sensor rather than the resistance of the individual beads.*

long-term stability; the typical resistance drift rate is only 0.025% per year. The packets are wired in parallel to reduce the overall resistance of the sensor. In addition, only one-third of the multimeter's excitation current $I_s$ passes through any given thermistor bead, minimizing the self-heating effect. To improve the ruggedness of the design, the thermistor packets are completely enclosed in a 4.0 mm diameter stainless-steel shell, allowing the probes to withstand the pressures encountered at 7–8 km in a liquid-filled borehole and the effects of corrosive chemicals such as n-butyl acetate. The use of many small thermistor beads, glass encapsulation and a high-conductivity steel shell all help to produce a high power-dissipation constant $\delta$. The $\delta$ value for our immersion probes is 55 mW K$^{-1}$ in circulating xylene; it is believed to be similar when logging through n-butyl acetate. The temperature coefficient $\alpha_T$ is temperature dependent, ranging from $-0.049$ K$^{-1}$ at $-10°$C to $-0.059$ K$^{-1}$ at $-40°$C. An inevitable disadvantage of this probe design is the relatively slow response time. In n-butyl acetate, the measured time constant is about 7 s. This slow response time means that measurements obtained in the continuous logging mode must be deconvolved in order to recover the actual borehole temperatures (Saltus and Clow, 1994), even when the logging speed is slow (e.g. 5 cm s$^{-1}$).

The probes we use to measure temperatures in air-filled holes are also custom-built. Reminiscent of the immersion probes, they consist of three rugged glass-encapsulated bead thermistors wired in parallel. The use of multiple beads yields a relatively high power-dissipation constant in still air, ($\delta \approx 3$ mW K$^{-1}$), limiting the self-heating effect to 0.7 mK under the worst conditions. The temperature coefficients $\alpha_T$ are virtually the same as for the immersion probes. Unfortunately, the time constant for these probes in air is long enough (90 s at sea level) to preclude their use in the continuous logging mode. Faster-responding air probes could be built but they would be more fragile, and would have higher long-term drift rates and larger self-heating effects.

To calibrate the probes, we insert them into a copper equilibration block that is immersed in a temperature-controlled fluid bath (Hart model 7041); the stability of the bath is estimated to be 0.5 mK. Reference

temperatures within the block are established on the ITS-90 temperature scale (Mangum and Furukawa, 1990) by monitoring a NIST-calibrated Standard Platinum Resistance Thermometer (SPRT) with an 8.5-digit multimeter while the probe resistances ($R_s$) are simultaneously measured using a 6.5-digit multimeter. The precision of the reference data from the SPRT is estimated to be 0.2–0.3 mK while the accuracy is 4.5 mK, traced to the U.S. National Institute for Science and Technology (NIST). For each temperature sensor, approximately 100 measurements of $R_s$ and $T$ are obtained at each of the calibration points, which are spaced every 5 K across the calibration range of $-40°$ to $+30°$C. The data acquired at each calibration point are subsequently averaged (in $(\ln R_s, 1/T)$ space) and the average values used to find the constants ($a_i$) in the four-term calibration function

$$T^{-1} = a_0 + a_1(\ln R_s) + a_2(\ln R_s)^2 + a_3(\ln R_s)^3, \quad (6)$$

using weighted least squares. Residuals from the least-squares fit are typically 0.3 mK, or less (Fig. 4). Equation (6) is an extension of the often-used three-term Steinhart–Hart equation (Steinhart and Hart, 1968), which proves inadequate for our purposes. An $F$ test (e.g. Bevington, 1969) demonstrates that a much better fit to our calibration data can be obtained with the four-term function (Equation (6)) than with the Steinhart–Hart equation, particularly at temperatures below 0°C.
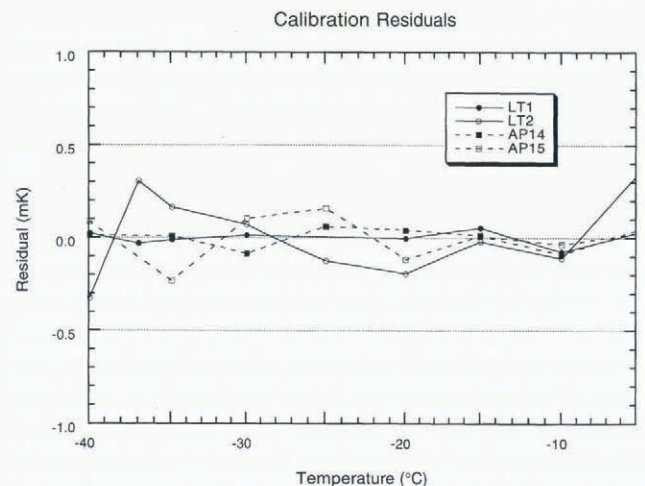


*Fig. 4. Residuals from the least-squares fit of the four-term calibration function to the calibration data for a typical pair of immersion probes (LT1, LT2) and a pair of air probes.*

**Depths**

Depth information is provided by an optical encoder that measures the rotation of one of the logging-cable pulleys. The encoder transmits information to a digital counter which in turn is connected to the system's computer using an RS-232 interface. With this system, the logging cable is tensioned before it enters the encoder pulley, so that cable stretch is automatically accounted for. However, cable slippage on the encoder pulley, thermal expansion or

contraction of the cable that has spooled past the pulley, or cable hang-ups in the hole can cause errors in the recorded location of the temperature probe while logging. These errors, although generally small, cannot be ignored.

A depth-calibration factor is derived for each logging cable by moving the sensor downhole approximately 40 m and comparing the output from the depth counter with that measured using a fiberglass tape measure that has a low coefficient of thermal expansion ($9.3 \times 10^{-6} \, K^{-1}$). This calibration procedure is performed several times with the cable under various tensions. Repeat calibrations and intercomparison with other depth measurements (i.e. total borehole depths determined from fluid-pressure measurements, from the measured lengths of ice cores, and from optical encoders on other logging systems) suggest that our accuracy is 2–3 m at a depth of 3 km. This 0.1% depth uncertainty introduces a 0.1% error in the temperature gradient calculated from the depth-temperature data.

## Measurement procedures

Before each experiment, the logging system's multimeter is brought to its operating temperature (22–24°C) and allowed to stabilize for at least 1 h. The DMM is then calibrated on site using a set of high-precision low-temperature-coefficient resistors that have also been maintained at 22–24°C for at least 1 h. Errors in the multimeter's calibration constants result in an uncertainty of $\approx 0.17$ mK in the subsequent temperature measurements. For deep boreholes such as GISP2, temperatures near the end of a logging experiment might not be acquired until up to 24 h after the multimeter has been calibrated. During this time, the multimeter's electronics may drift slightly. Based on the specifications of our present DMM (Analogic DP100), this drift can cause an uncertainty of up to 0.67 mK during the course of a long logging run. In practice, we find that our multimeter's 24 h drift is about one-quarter of the quoted specification.

## FIELD RESULTS

### GISP2, Greenland

During the boreal summers of 1994 and 1995, we used the new logging system to acquire temperature measurements in the 3 km deep borehole at GISP2; these measurements were obtained 12 and 24 months after the completion of the borehole, respectively. Experiments included continuous temperature logs, monitoring sessions at fixed depths to learn more about the convective behavior of the n-butyl acetate (Gosink and others, 1991) borehole fluid, and attempts to detect shear heating at the base of the ice sheet. All measurements in the deep hole were obtained using an immersion probe (USGS serial number LT1).

The logging system was configured identically during the 1994 and 1995 experiments except that a $10 \, \mu F$ capacitor was introduced between the high-impedance inputs of the DMM during 1994 to give additional high-frequency noise suppression. The resistance of probe LT1

ranged from 12.7 kΩ when near the surface to 3.8 kΩ as it approached the bottom of the hole, yielding a system sensitivity of 0.14–0.54 mK (Table 1). During the 1994 experiments, the resistance $R_l$ of one of the critical leakage paths was 5 GΩ; $R_l$ exceeded 20 GΩ for all other leakage paths during 1994 and for all the leakage paths during 1995. Thus, the inter-conductor leakage error $\epsilon_l$ was 0.016–0.045 mK during 1994 and was less than 0.011 mK during 1995. Circuit capacitance was $10 \, \mu F$ during 1994 and $0.63 \, \mu F$ during 1995, giving a circuit response time of 38–127 ms during 1994 and 2.4–8.0 ms during 1995. These response times were much faster than that of the sensor (7 s), allowing the circuit to detect any resistance changes experienced by the probe. With a logging speed of 5–6 cm s$^{-1}$ (continuous logs) and BT gradients of $-2$ to $+25$ mK m$^{-1}$, the temperature error $\epsilon_c$ due to the capacitance effect was less than 0.095 mK during 1994 and 0.003 mK during 1995. The source current $I_s$ of the multimeter was $10 \, \mu A$, limiting the self-heating effect $\epsilon_h$ to 0.007–0.023 mK. The bulk of this effect was corrected during data processing. System checks validated the stability of the electronics at the

*Table 1. Factors affecting the uncertainty of the processed temperature measurements from the 3 km GISP2 borehole*

| Source | Magnitude | |
|---|---|---|
| | July 1994 | June 1995 |
| | mK | mK |
| System sensitivity, $\Delta T$ | 0.14–0.54 | 0.14–0.54 |
| Inter-conductor leakage error, $\epsilon_l$ | 0.016–0.045 | <0.011 |
| Capacitance effect, $\epsilon_c$ | <0.095 | <0.003 |
| Self-heating effect, $\epsilon_h$ | <0.005 | <0.005 |
| Slip-ring noise, deconvolved | 0.25 | 0.34 |
| Probe calibration uncertainty | 0.15 | 0.15 |
| Multimeter calibration uncertainty | 0.18 | 0.18 |

level of the system's sensitivity.

During the continuous temperature logs, one measurement was acquired every 2.0 s, providing a sample spacing of 10–12 cm. Given the 7 s response time of the temperature sensor, the sampling rate was fast enough to prevent any aliasing of the temperature signal. At GISP2, we were able to position the logging system entirely within the protection of the drilling dome. Under these conditions, the high-frequency noise ($>0.025$ Hz) present in the raw data was due almost entirely to the slip-ring assembly (Fig. 5). For the 1994 (1995) log, the standard error of this noise is 0.50 mK (0.75 mK). Because of the relatively slow response time of the temperature sensor, the raw data must be deconvolved with the probe's response function to obtain the actual borehole temperatures from the continuous logs. This is done in two steps as described by Saltus and Clow (1994): (1) We
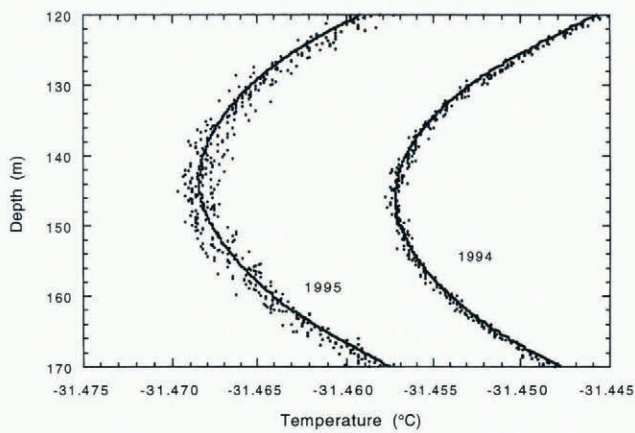
*Fig. 5. Detailed comparison of the continuous temperature logs obtained in the GISP2 borehole on 5 July 1994 and 14 June 1995 in the 120–170 m depth range. The high-frequency noise present in the raw data (dots) is primarily due to switching effects inside the slip-ring assembly. During data processing, the bulk of this noise is removed using optimal (Wiener) filtering. The filtered data are subsequently deconvolved to account for the finite response time of the moving sensor. The deconvolved signal (solid line) represents the actual temperatures in the borehole. For the 1994 log, a 10 μF capacitor was inserted between the high-impedance leads of the DMM to give additional high-frequency noise suppression.*

filter the high-frequency noise in the frequency domain using optimal (Wiener) filtering. Based on tests with synthetic data, the filtering effectively removes all noise at frequencies above the optimal filter cut-off and reduces the standard error of the noise to one-quarter of the original value at frequencies below the optimal smoothing cut-off. (2) The filtered data are deconvolved with the probe response function using serial division. The deconvolution process is very sensitive to any residual noise remaining in the filtered data. Based on synthetic test cases, we find that our deconvolution process amplifies the residual noise by a factor of 2. The net result is that the standard error of the residual slip-ring noise in the deconvolved data is 0.25 mK for the 1994 log and 0.34 mK for the 1995 log. This error controls the precision of the logs at depths above ∼2600 m while the system sensitivity, which degrades to 0.54 mK at the bottom of the hole, determines the precision for depths below about 2600 m. The accuracy of both the 1994 and 1995 logs is estimated to be 4.5 mK.

A great deal of heat was pumped into the GISP2 borehole during the 4 years it was being drilled. Upon completion of the borehole (July 1993), temperatures in the ice surrounding the upper section of the borehole are estimated to have been disturbed by roughly 100–200 mK. Simple heat-transfer models indicate it will be well into the next century before the borehole and surrounding ice return to thermal equilibrium. Figure 5 shows a detailed comparison of the 1994 and 1995 temperature logs in the 120–170 m depth range. The data quality is high enough to show the borehole had cooled 10–13 mK at these shallow depths during the 344 d separating the two logs. At depths exceeding 400 m, the

initial drilling disturbance is expected to have been much less, and the observed cooling between the 1994 and 1995 logs is indeed less than 2 mK.

Based on the calculated Rayleigh numbers for the GISP2 borehole (Clow and others, 1995), we expected the borehole fluid to be convecting below a depth of 1600 m where the temperature gradient exceeds $1.46\,\mathrm{mK\,m^{-1}}$; the convection was expected to be laminar in the 1600–2000 m depth zone and turbulent below 2000 m. Figures 6–8 show some of the data we obtained in an effort to verify these predictions. A monitoring experiment at 1520 m (Fig. 6) shows no evidence of convection, at least at the level of the system's sensitivity at this depth (0.14 mK). Within the fully turbulent zone, a similar experiment reveals rapid temperature excursions of up to 20 mK due to the passage of energetic convective eddies (Fig. 7). Convection cells can also be seen in the continuous log. Figure 8 shows a detailed section of the 5 July 1994 temperature log in the laminar zone. Convective cells with wavelengths of 3–5 m and amplitudes of 1–2 mK are readily apparent in this zone.
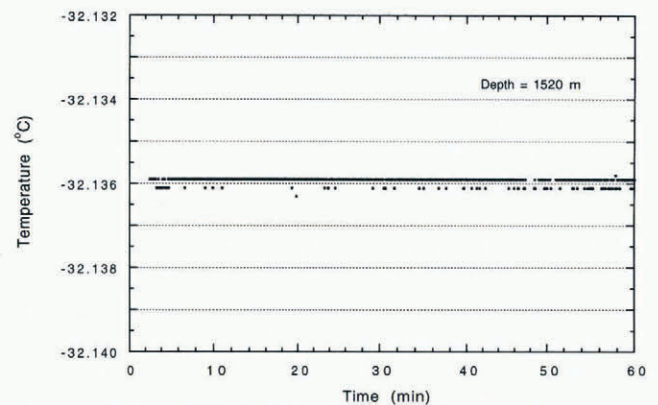


*Fig. 6. Monitoring experiment at 1520 m in the GISP2 borehole. At this depth, no evidence of convection is apparent at the limit of our sensitivity, 0.14 mK. This experiment also demonstrates the stability of the electronics package.*
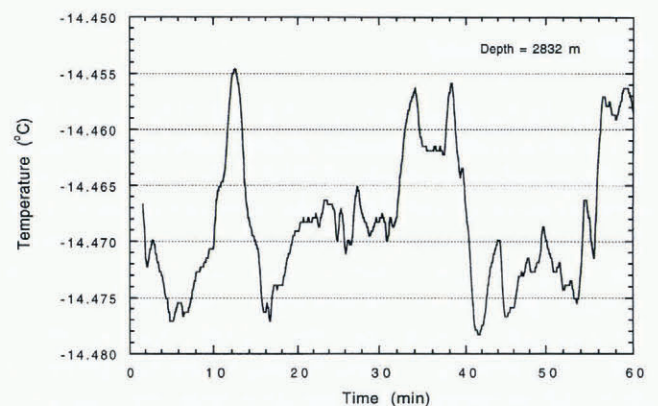


*Fig. 7. Monitoring experiment at 2832 m in the GISP2 borehole. This data was acquired within the fully turbulent zone of the borehole. Rapid temperature fluctuations associated with energetic convective eddies are readily detected.*
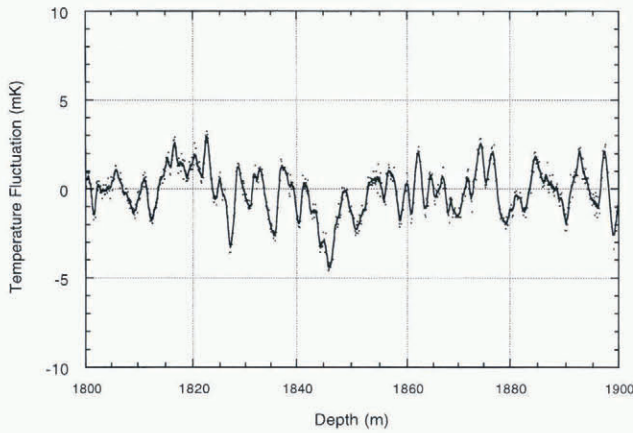
*Fig. 8. Convection cells are apparent in the GISP2 continuous log below 1600 m. Here, we show the temperature fluctuations about the local trend resulting from laminar convection in the 1800–1900 m depth range (5 July 1994). The raw data are represented by dots while the solid line shows the deconvolved signal.*

## Taylor Dome, Antarctica

During the 1994–95 austral field season, we made temperature measurements in the newly completed 554 m butyl-filled borehole at Taylor Dome on the Antarctic Polar Plateau (Grootes and others, 1994). The system's characteristics were similar to those reported in the previous section. In conjunction with logging the 554 m borehole, we also incrementally logged an air-filled 130 m hole (TD-C) that had been cored adjacent to the deep hole. These measurements were obtained using one of our three-bead "air" probes.

Prior to logging the TD-C hole, we cased the upper 2 m of the hole using 15 cm PVC pipe. Our nylon equipment shelter was then placed over the borehole. Although the top of the casing was sealed during the subsequent temperature measurements, we believe the seal was imperfect, allowing atmospheric-pressure changes to influence the temperatures in the borehole. With firn temperatures close to −40°C, the resistance of the temperature sensor (USGS serial number AP14) ranged from 16.1 kΩ at the top of the hole to 13.5 kΩ at the bottom. Under these conditions, the system's sensitivity was 0.11–0.13 mK (Table 2). Critical leakage paths had

*Table 2. Factors affecting the uncertainty of the processed temperature measurements from the air-filled 130 m hole at Taylor Dome, Antarctica*

| Source | Magnitude mK |
|---|---|
| System sensitivity, $\Delta T$ | 0.11–0.13 |
| Inter-conductor leakage error, $\epsilon_l$ | 0.026 |
| Self-heating effect, $\epsilon_h$ | < 0.17 |
| Wind-related noise | < 0.32 |
| Probe calibration uncertainty | 0.3 |
| Multimeter calibration uncertainty | 0.17 |

resistances of ∼10 GΩ, yielding an inter-conductor leakage error $\epsilon_l$ of 0.026 mK. The self-heating effect $\epsilon_h$ was 0.51 mK; after data processing, the magnitude of the self-heating error is estimated to be less than 0.17 mK. Although the entire logging system was operated within the protection of the instrument tent, some noise is evident in the data acquired on windy days. This is most likely due to static-charge build-up on the tent. The magnitude of the wind-related noise ranged from 0.18–0.32 mK on moderately windy days (wind speeds of 5–7 m s$^{-1}$) to < 0.11 mK on calm days (wind speeds < 3 m s$^{-1}$). Taking into account the various sources of error, the overall precision of the processed data is 0.11 mK for the data acquired on calm days. The precision degrades to 0.32 mK for data acquired when wind speeds approached 7 m s$^{-1}$. In both cases, the accuracy of the temperature measurements is 4.5 mK. Because the atmospheric pressure at Taylor Dome (elevation ≈ 2425 m) is low relative to sea level, the response time of our three-bead "air" probe was expected to be slower than its nominal sea-level value, 90 s. Response tests established that the time constant for air probe AP14 is 260 s when used at Taylor Dome.

Figures 9 and 10 show some of the data we obtained in the TD-C borehole. Strong temperature oscillations with standard errors of 20–30 mK were observed while incrementally logging in the 10–12 m depth range. These oscillations progressively diminished with depth, dropping below ±1.0 mK at about 65 m. By simultaneously monitoring atmospheric-pressure changes with a transducer buried 1 m below the surface of the snow (the open port was 10 cm below the snow's surface), we found that the temperature fluctuations in the borehole correlated well with atmospheric-pressure changes, at least on time-scales exceeding 260 s (Fig. 9). Even at 49 m where the standard error of the oscillations was only 1.1 mK, both the short-term temperature fluctuations and the multi-hour trends were found to correlate with atmospheric-pressure changes (Fig. 10). Thus, the temperature
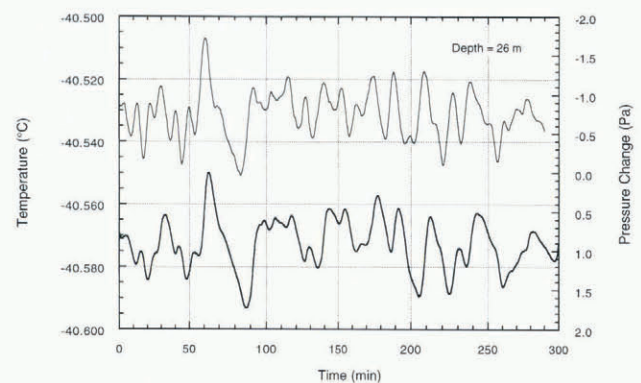


*Fig. 9. Temperatures recorded at 26 m while incrementally logging the 130 m air-filled hole at Taylor Dome, Antarctica (lower curve). Atmospheric-pressure changes (upper curve) were simultaneously recorded 10 cm below the surface of the snow adjacent to the borehole. The temperature fluctuations observed in the borehole correlate well with changes in atmospheric pressure. To match the response time of the temperature sensor, the pressure data have been smoothed using a 260 s moving average.*
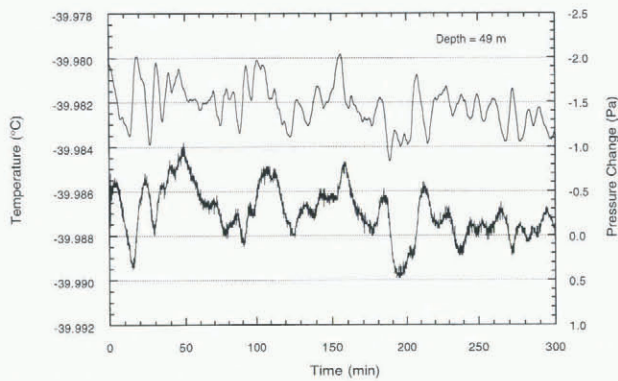
*Fig. 10. Same experimental set-up as for Figure 9 except for temperatures recorded at 49 m in the TD-C borehole. Again, the temperature and pressure fluctuations are correlated, as are the multi-hour trends. The high-frequency noise (standard error ≈0.10 mK) in the temperature data is due to static-charge build-up on the instrument tent which was exposed to dry wind-blown snow. These data were acquired on a relatively calm day.*

fluctuations and trends that we observed in the air-filled TD-C borehole down to the milli-Kelvin level are real.

## CONCLUDING REMARKS

It is currently possible to make BT measurements with precisions of 0.1–1.0 mK. To achieve this, the interaction of the measuring circuit and the probe must be carefully considered in order to optimize the system's sensitivity while minimizing sources of instrumental error (e.g. inter-conductor leakage and self-heating effects). Calibration and other operational procedures must also be carefully considered. The "slip-ring" noise produced during continuous logs can be substantially removed through optimal (Wiener) filtering. Although the deconvolution process used to remove the effect of a temperature sensor's relatively slow response time does amplify the random noise, it is still possible to attain a precision better than 1 mK for processed continuous temperature logs. The availability of data with this precision should allow a marked improvement in the accuracy of past climate (surface-temperature) reconstructions based on BT measurements. In addition, several effects that influence the interpretation of the BT measurements can be detected and quantified. These effects include: the thermal disturbance in the ice surrounding a borehole caused by drilling operations, fluid convection within a liquid-filled borehole, and pressure-induced temperature fluctuations in air-filled boreholes. Temperature measurements with precisions in the 0.1–1.0 mK range may also help us better quantify various heat-source and heat-transfer mechanisms in ice sheets. This in turn will lead to improved ice-sheet models. Under conditions similar to those encountered at GISP2, Greenland, and Taylor

Dome, Antarctica, the precision of the data produced by the USGS logging system is typically 0.1–0.4 mK while the accuracy is ~4.5 mK.

## REFERENCES

Alley, R.B. and B.R. Koci. 1989. Recent warming in central Greenland? *Ann. Glaciol.*, **14**, 6–8.

Beck, A.E. and N. Balling. 1988. Determination of virgin rock temperatures. *In* Haenel, R., L. Rybach and L. Segena, *eds. Handbook of terrestrial heat-flow density determination*. Dordrecht, Kluwer Academic Publishing, 59–85.

Bevington, P.R. 1969. *Data reduction and error analysis for the physical sciences*. New York, McGraw-Hill.

Clow, G.D. 1992. The extent of temporal smearing in surface-temperature histories derived from borehole temperature measurements. *Palaeogeogr., Palaeoclimatol., Palaeoecol.*, **98**, 81–86.

Clow, G.D., R.W. Saltus and E.D. Waddington. 1995. High-precision temperature logging at GISP2, Greenland, May 1992. *U.S. Geol. Surv. Open-File Rep.* 95-490.

Dahl-Jensen, D. and S. Johnsen. 1986. Palaeotemperatures still exist in the Greenland ice sheet. *Nature*, **320**(6059), 250–252.

Dansgaard, W., S.J. Johnsen, H.B. Clausen and N. Gundestrup. 1973. Stable isotope glaciology. *Medd. Grønl.*, **197**(2), 1–53.

Firestone, J. 1995. Resolving the Younger Dryas event through borehole thermometry. *J. Glaciol.*, **41**(137), 39–50.

Gosink, T.A., J.J. Kelley, B.R. Koci, T.W. Burton and M.A. Tumeo. 1991. Butyl acetate, an alternative drilling fluid for deep ice-coring projects. *J. Glaciol.*, **37**(125), 170–176.

Grootes, P.M., E.J. Steig and M. Stuiver. 1994. Taylor ice dome study 1993–1994: an ice core to bedrock. *Antarct. J. U.S.*, **29**(5), 79–81.

Keithley, J.F. 1984. *Low level measurements for effective low current, low voltage, and high impedance measurements*. Cleveland, OH, Keithley Instruments Inc.

MacAyeal, D., J. Firestone and E.D. Waddington. 1991. Paleothermometry by control methods. *J. Glaciol.*, **37**(127), 326–338.

Mangum, B.W. and G.T. Furukawa. 1990. *Guidelines for realizing the International Temperature Scale of 1990 (ITS-90)*. Gaithersburg, MD, U.S. National Institute of Standards and Technology. (NIST Technical Note 1265.)

Saltus, R.W. and G.D. Clow. 1994. Deconvolution of continuous borehole temperature logs. Example from the Greenland GISP2 icecore hole. *U.S. Geol. Surv. Open-File Rep.* 94-254.

Sass, J.H., A.H. Lachenbruch, R.J. Munroe, G.W. Greene and T.H. Moses, Jr. 1971. Heat flow in the western United States. *J. Geophys. Res.*, **76**(26), 6376–6413.

Shen, P.Y. and A.E. Beck. 1991. Least squares inversion of borehole temperature measurements in functional space. *J. Geophys. Res.*, **96**(B12), 19,965–19,979.

Steinhart, J.S. and S.R. Hart. 1968. Calibration curves for thermistors. *Deep-Sea Res.*, **15**(4), 497–503.

Wang, K. 1992. Estimation of ground surface temperatures from borehole temperature data. *J. Geophys. Res.*, **97**(B2), 2095–2106.